IMPROVED CONTROL SCHEME OF DFIG WIND TURBINE SYSTEMS UNDER UNBALANCED GRID VOLTAGE

Van Tan Luong[1*], Phan Thi Chieu My[2], Duong Van Khai[1]
[1]*Ho Chi Minh City University of Food Industry*
[2]*Van Hien University*
*Email: *luonghepc@gmail.com*
Received: 28 September 2018; Accepted for publication: 05 December 2018

ABSTRACT

This paper proposes an enhanced nonlinear control technique based on a combination of feedback linearization (FBL) and resonant regulator as tracking controllers for the doubly-fed induction generator (DFIG) wind turbine system under unbalanced grid voltage. A nonlinear model of DFIG wind turbine system with the rotor-side converter (RSC) is firstly linearized, not by small signal analysis. Then, the proportional integral plus resonant (PI+R) regulators are utilized for tracking controller. With the combination of FBL technique and the tracking controllers based on resonant regulator, the oscillations of the power and generator torque can be much reduced in the transient and steady states. The effectiveness of the proposed scheme is verified by the simulation results for the 2 MW-DFIG wind turbine system under unbalanced grid voltage conditions.

Keywords: Current control, doubly-fed induction generator, feedback linearization theory, unbalanced grid voltage, wind turbine.

1. INTRODUCTION

Nowadays, many speed variable wind turbines (WT) are based on DFIGs, which are connected to the grid through back to back converters. The major advantage of these facilities lies in the fact that the power rate of the inverters is around the 25-30% of the rated generator power. This feature permits to regulate the electrical power production within this range, something that has been proven to be a good trade-off between the optimal operation and costs.

The performance of the wind turbine system with DFIG under normal conditions is currently well understood [l, 2]. Practically, both transmission and distribution networks can have voltage imbalance. As for the induction generators, if the voltage unbalance is not considered by the control system, the current could be highly unbalanced even with a small unbalanced stator voltage. The unbalanced currents cause unequal heating on the stator windings [3]. The heat may increase the winding temperature, which degrades the insulation of the winding, i.e., the life expectancy of the winding. Also, unbalanced currents create torque pulsation on the shaft resulting in audible noise and extra mechanical stress. A wind turbine based on DFIG without unbalanced voltage control might be disconnected from the grid during the network voltage unbalance [4]. On the other hand, grid codes are required for wind farms to withstand a small 2% steady-state voltage unbalance and larger transient voltage unbalance without tripping [5].

Several various methods have been suggested to control the current of the generator under unbalanced grid conditions [6-10]. As suggested by Lopez *et al*., Brekken *et al*., Abo-Khalil *et al*. and Hu *et al*., the positive and negative proportional-integral (PI) current controllers in synchronous d-q axis, and the positive and negative the proportional resonant (PR) current controller in the stationary α-β axis have been introduced in detail [6-9]. However, both current controllers could not eliminate the non-linearity of the DFIG. A nonlinear control with feedback linearization method was introduced for DFIG [10, 11]. In this method, the tracking controllers based on the PI regulators after linearizing the nonlinear model of the DFIG wind power system by the FBL technique was used to eliminate the steady-state errors. Under unbalanced grid voltages, the FBL with PI tracking controllers fails to eliminate the steady-state errors completely, since the controlled variables contain AC signals.

To overcome the drawback of the aforementioned feedback linearization control with the steady-state error for AC controlled variables, an enhanced control strategy for the DFIG wind power system is proposed in this paper, where a combination of the FBL with the PI plus R regulator is employed. The FBL technique is used to linearize the nonlinear model of the DFIG wind power system working in the grid fault conditions. Thus, the nonlinear controller designed becomes simpler and gives the fast performances of the system, compared with the dual PI current controllers. Simulation results for a 2 MW-DFIG wind turbine system are provided to verify the validity of the proposed control scheme.

2. BEHAVIORS OF DFIG UNDER UNBALANCED VOLTAGE CONDITIONS

Figure 1 shows the variable vector *F* between the $\alpha_s\beta_s$, $\alpha_r\beta_r$ and dq^+, dq^-. For a vector *F*, the transformations between different reference frames are given as

$$\begin{aligned} F_{dq}^{+} &= F_{\alpha\beta}^{s} e^{-j\omega_e t}, \quad F_{dq}^{-} = F_{\alpha\beta}^{s} e^{j\omega_e t} \\ F_{dq}^{+} &= F_{dq}^{-} e^{-j2\omega_e t}, \quad F_{dq}^{-} = F_{dq}^{+} e^{j2\omega_e t} \\ F_{dq}^{+} &= F_{\alpha\beta}^{r} e^{-j(\omega_e-\omega_r)t}, \quad F_{dq}^{-} = F_{\alpha\beta}^{r} e^{j(-\omega_e-\omega_r)t} \end{aligned} \tag{1}$$

where *F* represents voltage, current and flux.

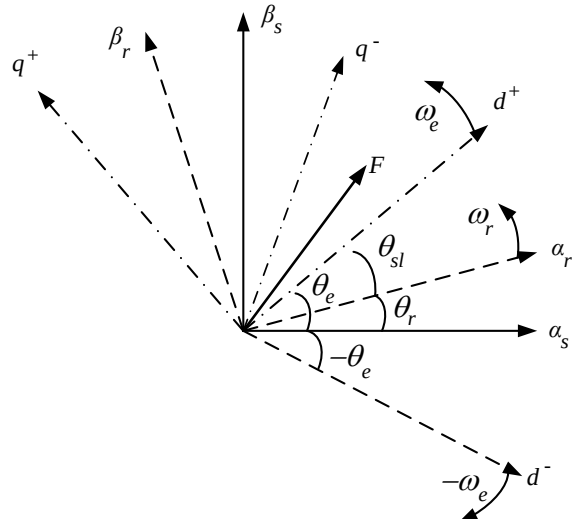

Figure 1. Relation between the $\alpha_s\beta_s$, $\alpha_r\beta_r$ and dq^+, dq^- reference frames.

During the voltage unbalance, the voltage, current, and flux all contain positive- and negative-sequence components. Based on equation (1) and shown in Figure 1, F can be expressed in terms of positive- and negative-sequence components in the respective positive and negative rotating synchronous frames as

$$F_{dq} = F_{dq}^{+} + F_{dq}^{-} e^{-j2\omega_e t} \tag{2}$$

It is seen in (2) that the dq-axis components contain the second-order oscillation component.

Under unbalanced voltage conditions, the rotor voltage equations of DFIG in the dq^{+} reference frame can be expressed as [10]

$$V_{dr}^{+} = R_r I_{dr}^{+} + \sigma L_r \frac{dI_{dr}^{+}}{dt} - (\omega_s - \omega_r)\frac{L_m}{L_s}\lambda_{qs}^{+} - (\omega_s - \omega_r)\sigma L_r I_{qr}^{+} \tag{3}$$

$$V_{qr}^{+} = R_r I_{qr}^{+} + \sigma L_r \frac{dI_{qr}^{+}}{dt} + (\omega_s - \omega_r)\frac{L_m}{L_s}\lambda_{ds}^{+} + (\omega_s - \omega_r)\sigma L_r I_{dr}^{+} \tag{4}$$

where $\sigma L_r = L_r - \dfrac{L_m^2}{L_s L_r}$

In equations (3) and (4), the nonlinear state-space model of the rotor side of DFIG is represented by

$$\begin{bmatrix} \dot{I}_{dr}^{+} \\ \dot{I}_{qr}^{+} \end{bmatrix} = \begin{bmatrix} A \\ B \end{bmatrix} + \begin{bmatrix} \dfrac{1}{\sigma L_r} & 0 \\ 0 & \dfrac{1}{\sigma L_r} \end{bmatrix} \begin{bmatrix} V_{dr}^{+} \\ V_{qr}^{+} \end{bmatrix} \tag{5}$$

where

$$A = \frac{-R_r}{\sigma L_r} I_{dr}^{+} + (\omega_s - \omega_r) I_{qr}^{+}$$

$$B = \frac{-R_r}{\sigma L_r} I_{qr}^{+} - (\omega_s - \omega_r)\frac{L_m^2 I_{ms}^{+}}{\sigma L_r L_s} - (\omega_s - \omega_r) I_{dr}^{+}$$

Under unbalanced voltage condition, the instantaneous active and reactive stator powers are expressed as [8, 10]

$$p_s(t) = P_{s0} + P_{sc2}\cos(2\omega_e t) + P_{ss2}\sin(2\omega_e t) \tag{6}$$

$$q_s(t) = Q_{s0} + Q_{sc2}\cos(2\omega_e t) + Q_{ss2}\sin(2\omega_e t) \tag{7}$$

where

$$\begin{bmatrix} P_{s0} \\ Q_{s0} \\ P_{ss2} \\ P_{sc2} \\ Q_{ss2} \\ Q_{sc2} \end{bmatrix} = \frac{3}{2\omega_e L_s} \begin{bmatrix} 0 & 0 & 0 & 0 \\ V_{qs}^{+} & -V_{ds}^{+} & -V_{qs}^{-} & -V_{ds}^{-} \\ -V_{qs}^{-} & -V_{ds}^{-} & -V_{qs}^{+} & -V_{ds}^{+} \\ -V_{ds}^{-} & V_{qs}^{-} & V_{ds}^{+} & -V_{qs}^{+} \\ 0 & 0 & 0 & 0 \\ 0 & 0 & 0 & 0 \end{bmatrix} \begin{bmatrix} V_{qs}^{+} \\ V_{ds}^{+} \\ V_{qs}^{-} \\ V_{ds}^{-} \end{bmatrix} + \frac{3L_m}{2L_s} \begin{bmatrix} V_{ds}^{+} & V_{qs}^{+} & V_{ds}^{-} & V_{qs}^{-} \\ V_{qs}^{+} & -V_{ds}^{+} & V_{qs}^{-} & -V_{ds}^{-} \\ V_{qs}^{-} & -V_{ds}^{-} & -V_{qs}^{+} & V_{ds}^{+} \\ V_{ds}^{-} & V_{qs}^{-} & V_{ds}^{+} & V_{qs}^{+} \\ -V_{ds}^{-} & -V_{qs}^{-} & V_{ds}^{+} & V_{qs}^{+} \\ V_{qs}^{-} & -V_{ds}^{-} & V_{qs}^{+} & -V_{ds}^{+} \end{bmatrix} \begin{bmatrix} I_{dr}^{+} \\ I_{qr}^{+} \\ I_{dr}^{-} \\ I_{qr}^{-} \end{bmatrix} \tag{8}$$

The current reference of the rotor-side converter compensating for the stator active and reactive power ripples can be derived as

$$\begin{bmatrix} I_{dr}^{+*} \\ I_{qr}^{+*} \\ I_{dr}^{-*} \\ I_{qr}^{-*} \end{bmatrix} = \begin{bmatrix} V_{ds}^{+} & V_{qs}^{+} & V_{ds}^{-} & V_{qs}^{-} \\ V_{qs}^{+} & -V_{ds}^{+} & V_{qs}^{-} & -V_{ds}^{-} \\ V_{qs}^{-} & -V_{ds}^{-} & -V_{qs}^{+} & V_{ds}^{+} \\ V_{ds}^{-} & V_{qs}^{-} & V_{ds}^{+} & V_{qs}^{+} \\ -V_{ds}^{-} & -V_{qs}^{-} & V_{ds}^{+} & V_{qs}^{+} \\ V_{qs}^{-} & -V_{ds}^{-} & V_{qs}^{+} & -V_{ds}^{+} \end{bmatrix}^{-1} \cdot \frac{2L_s}{3L_m} \left(\begin{bmatrix} P_{s0} \\ Q_{s0} \\ P_{ss2} \\ P_{sc2} \\ Q_{ss2} \\ Q_{sc2} \end{bmatrix} - \frac{3}{2\omega_e L_s} \begin{bmatrix} 0 & 0 & 0 & 0 \\ V_{qs}^{+} & -V_{ds}^{+} & -V_{qs}^{-} & -V_{ds}^{-} \\ -V_{qs}^{-} & -V_{ds}^{-} & -V_{qs}^{+} & -V_{ds}^{+} \\ -V_{ds}^{-} & V_{qs}^{-} & V_{ds}^{+} & -V_{qs}^{+} \\ 0 & 0 & 0 & 0 \\ 0 & 0 & 0 & 0 \end{bmatrix} \begin{bmatrix} V_{qs}^{+} \\ V_{ds}^{+} \\ V_{qs}^{-} \\ V_{ds}^{-} \end{bmatrix} \right) \quad (9)$$

where P_{s0} means the power reference which is obtained from the maximum power point tracking method.

3. PROPOSED CONTROL SCHEME USING A COMBINATION OF FEEDBACK LINEARIZATION AND RESONANT REGULATOR

The fundamental principle of using the FBL technique is to linearize the nonlinear system by differentiating the outputs of the system until the input variables appear [11-14].

A multi-input multiple-output (MIMO) system can be considered as follows:

$$\dot{x} = f(x) + gu \quad (10)$$

$$y = h(x) \quad (11)$$

where x is the state vector, u is the control input, y is the output, f and g are the smooth vector fields, respectively, and h is the smooth scalar function.

The nonlinear model of the DFIG at the rotor side in (3) and (4) is expressed in (10) and (11) as: $x = \begin{bmatrix} I_{dr}^{+} & I_{qr}^{+} \end{bmatrix}^T ; u = \begin{bmatrix} V_{dr}^{+} & V_{qr}^{+} \end{bmatrix}^T ; y = h(x) = \begin{bmatrix} I_{dr}^{+} & I_{qr}^{+} \end{bmatrix}^T$

An approach to obtain the input–output linearization of the MIMO system is to differentiate the output y of the system until input control signal appears. The result is given as

$$\dot{y} = f(x) + gu \quad (12)$$

If a control input u is chosen as

$$u = g^{-1}\left[-f(x) + v \right] \quad (13)$$

where v is the equivalent control input to be specified. The resultant dynamics become linear as

$$\dot{y} = v = \begin{bmatrix} v_1 \\ v_2 \end{bmatrix} \quad (14)$$

Under the grid fault conditions, the rotor currents of the DFIG may contain the DC, and second-order oscillation component as seen in (2). Thus, the proportional integral plus resonant regulators are employed for the tracking controllers to eliminate the steady-state errors. For tracking the references of the dq-axis components, the central frequency of the resonant regulators are chosen at a second order ($2\omega_e$) with the aim of obtaining an infinite gain at this resonant frequency. Therefore, the new control inputs can be rewritten in the

Laplace domain as

$$\begin{bmatrix} v_1 \\ v_2 \end{bmatrix} = \begin{bmatrix} sy_1^* - k_{11}e_1 - k_{12}\dfrac{e_1}{s} - k_{13}\dfrac{s}{s^2+(2\omega_e)^2}e_1 \\ sy_2^* - k_{21}e_2 - k_{22}\dfrac{e_2}{s} - k_{23}\dfrac{s}{s^2+(2\omega_e)^2}e_2 \end{bmatrix} \tag{15}$$

where $e_1 = y_1^* - y_1$ and $e_2 = y_2^* - y_2$, y_1^* and y_2^*, are the reference values of the y_1 and y_2, respectively, k_{11}, k_{12}, k_{13}, k_{21}, k_{22} and k_{23} are the gains of tracking controller.

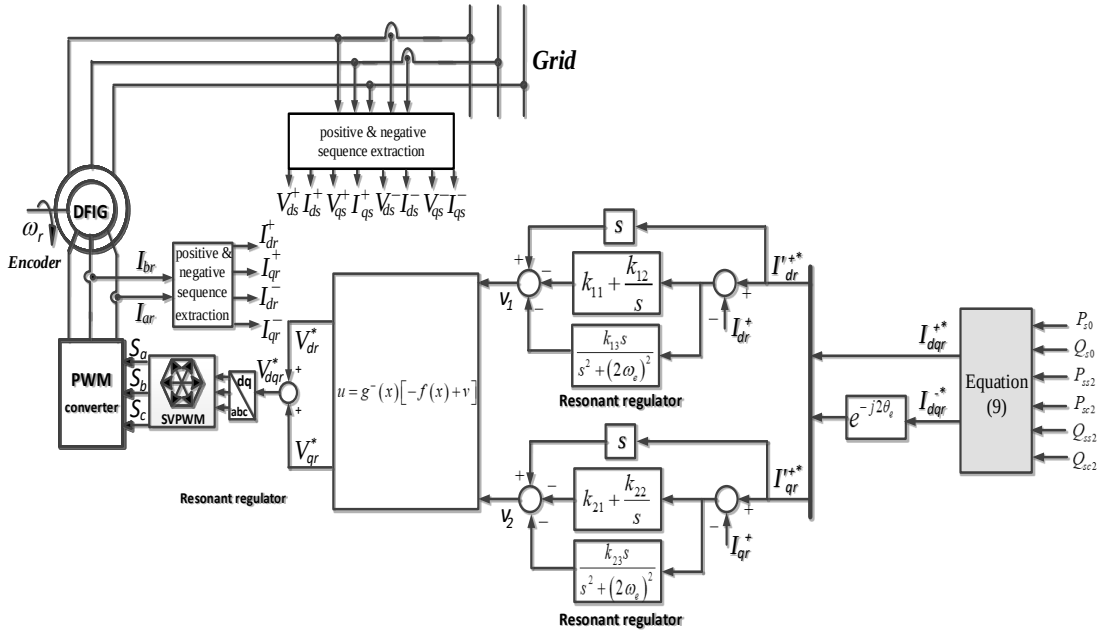

Figure 2. Proposed control block diagram of DFIG.

The block diagram of the proposed control is shown in Figure 2, in which the components of the positive-sequence rotor currents in dq-axis are separately controlled by the combination of the FBL technique and PI+R. It is noted that, in this work the second order component of the frequency in the system are only taken into account, which is added in the new control inputs in (15). Then, the FBL control outputs, V_{dr}^*, V_{qr}^* are transformed to the voltage references in three-phase abc frame, which are modulated by the space vector pulse-width modulation (SVPWM).

The tracking errors can be successfully converged to zero when the gains of tracking controllers are properly designed. A pole-placement technique is commonly used to obtain the gains. It is assumed that the resonant regulator with a resonant frequency of $2\omega_e$ is considered for deriving the closed-loop transfer function of the d-axis positive-sequence current tracking controller and its plant, $G_d(s)$. The closed-loop transfer functions of the q-axis positive-sequence current tracking controllers and its plants are derived in the same way. A pole placement technique is used to place all poles of the system at specific locations in the left-half side of the complex plane resulting in a stable system, which then the poles are chosen as $s_1 = -50$, $s_2 = s_3 = -250$ and $s_4 = 294{,}4$ by a trial-and-error method with a consideration of satisfactory performance in terms of the percent overshoot, settling time, and rise time.

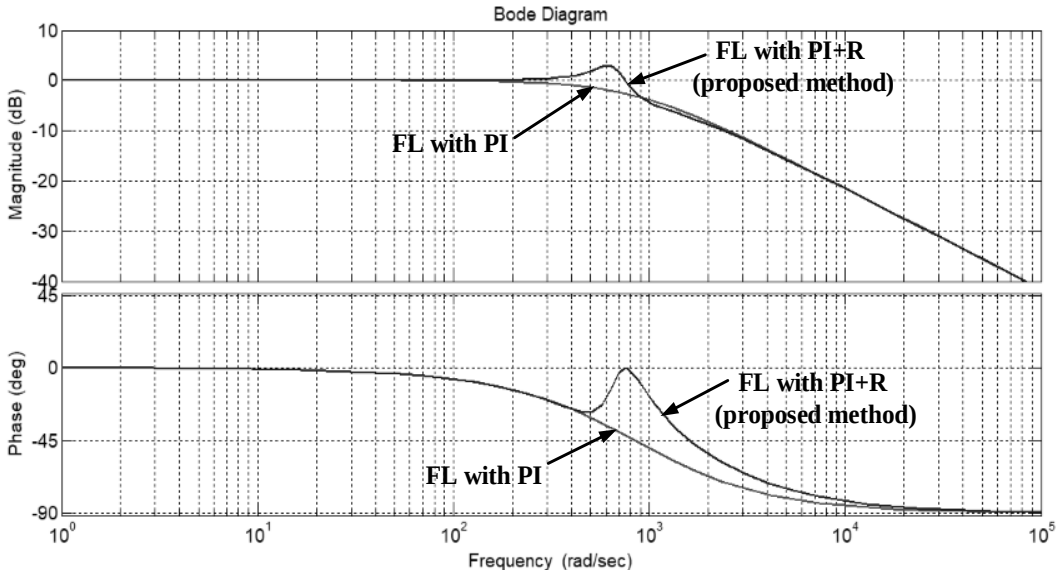

Figure 3. Bode plots for the FBL with tracking controllers of PI and PI+R.

In order to investigate the superior characteristics of the FBL with PI+R tracking controller (proposed controller) over the FBL with PI tracking controller (conventional controller), Figure 3 describes closed-loop Bode diagram for the conventional controller and the proposed controller given in (16) and (17), respectively.

$$G_{d1}(s) = \frac{k_{11}s + k_{12}}{s^2 + k_{11}s + k_{12}} \tag{16}$$

$$G_d(s) = \frac{k_{11}s^3 + (k_{12} + k_{13})s^2 + 4\omega^2 k_{11}s + 4\omega^2 k_{12}}{s^4 + k_{11}s^3 + (k_{12} + k_{13} + 4\omega^2)s^2 + 4\omega^2 k_{11}s + 4\omega^2 k_{12}} \tag{17}$$

$$k_{11} = -(s_1 + s_2 + s_3 + s_4)$$

$$k_{12} = -\frac{s_1 s_2 s_3 s_4}{4\omega^2}$$

$$k_{13} = s_1 s_2 + s_2 s_3 + s_3 s_4 - 4\omega^2$$

As shown in Figure 3, the FBL with PI+R tracking controller including the resonant frequency of $2\omega_e$ produces very high gains for ensuring zero steady-state errors in compensating the current oscillation. If the resonant regulators at $2\omega_e$ are added in (15), then the dynamic performance of the FBL with PI+R tracking controller will be satisfied with a unity gain and low phase shift for the resonant frequency. In addition, as illustrated in Figure 3, the FBL with PI+R tracking controller has a wide bandwidth than that of the FBL with PI tracking controller.

4. SIMULATION RESULTS

PSCAD simulation has been carried out for a 2 MW-DFIG wind turbine system to verify the feasibility of the proposed method. For the wind turbine: R = 44 m; ρ = 1,225 kg/m^3; λ_{opt} = 8, $J_t = 5{,}67 \times 10^6$ kg·m^2; and the wind speed is constant at 10 m/s. For the DFIG: the grid voltage is 690 V/60 Hz; the rated power is 2 MW; R_s = 0,00488 pu; R_r = 0,00549 pu; L_{ls} = 0,0924 pu; L_{lr} = 0,0995 pu; and J_g = 200 kg·m^2. The grid voltage is 690 V and 60 Hz.

Figure 3 shows the system performance for a grid unbalanced voltage sag. The wind speed is assumed to be constant (10 m/s) since the wind speed variations cannot produce a remarkable effect during the short time duration of the fault. The fault condition is 12% sag in the grid A-phase voltage for 0,5 s which is between 1,5 s and 2 s. Figure 3A shows the performance of the DFIG wind turbine system using the FBL with PI tracking controller, in case of the unbalanced grid condition. As can be seen from Figure 3A(c), the positive-sequence rotor currents in d-and q-axis become large. Likewise, the stator active power, stator reactive power and the generator torque contain the significant pulsations at 120 Hz. The generator torque which is shown in Figure 3A (f) is much increased during the grid fault.

Figure 3B shows the DFIG performance using the FBL with PI+R tracking controller for the rotor currents at the rotor-side converter under the grid fault condition. With the current control based on combination of FBL technique and the resonant regulator, the positive-sequence rotor current ripples in d-and q-axis as shown in Figure 3B (c) are suppressed. Accordingly, the ripples of the stator active and reactive powers are also mitigated, as shown in Figure 3B (d) and Figure 3B (e), respectively. Also, the generator torque ripples as shown in Figure 3B (f) are significantly reduced.

Figure 4 shows the system performance for grid unbalanced voltage sags which are 12% for A-phase and B-phase voltages during 0,5 s. With the combination of FBL technique and the tracking controllers based on resonant regulator, the ripples of the positive-sequence rotor current in d-and q-axis as shown in Figure 4B (c) are much reduced. Also, the stator active power and reactive power ripples are also suppressed, as shown in Figure 4B (d) and 4B (e), respectively. In addition, the generator torque ripples as shown in Figure 4B (f) are considerably mitigated, compared with the the FBL with PI tracking controller.

By comparison, the FBL with PI+R tracking controller gives smaller ripples than the FBL with PI tracking controller.

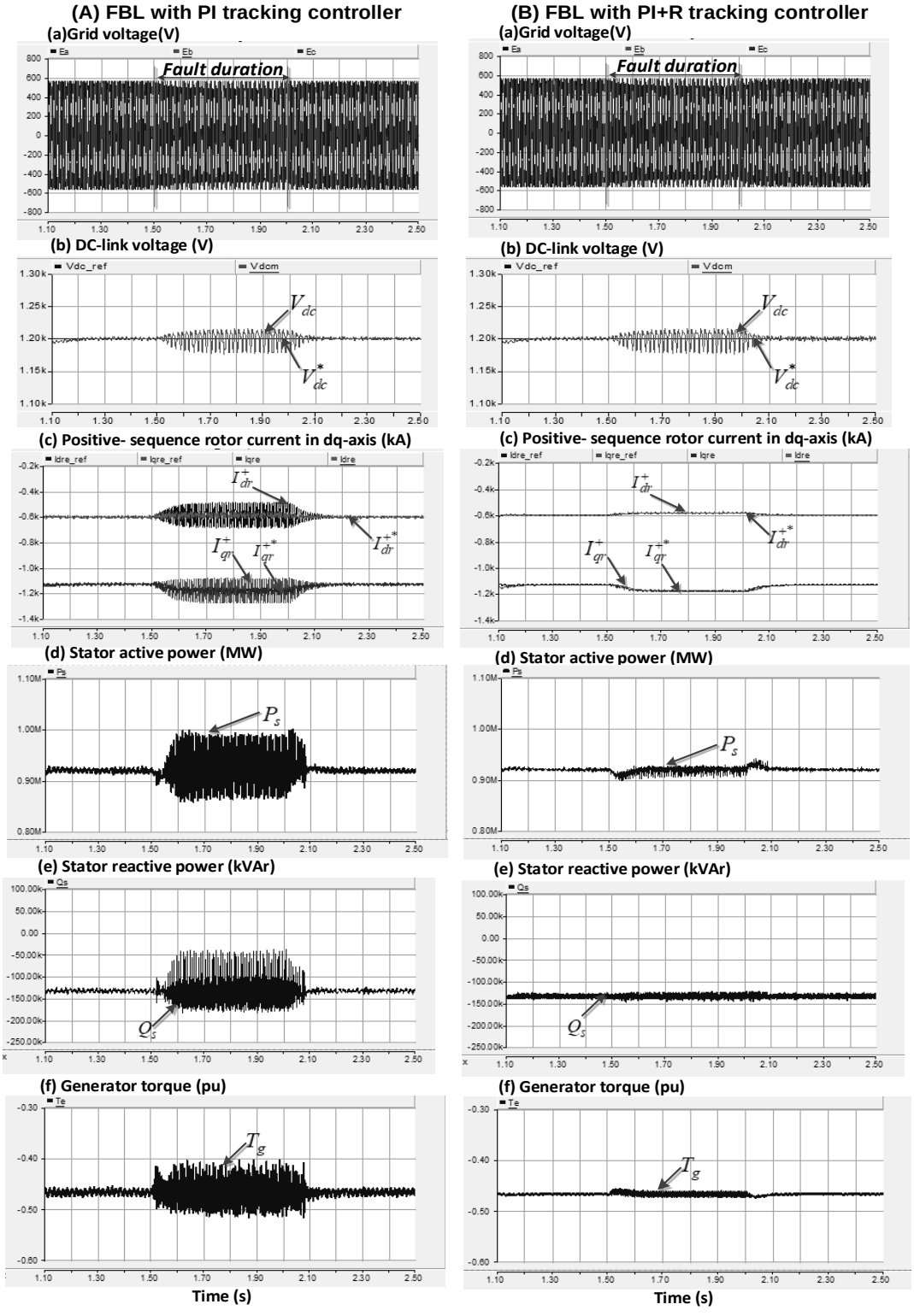

Figure 3. Wind generation performance for grid phase-A voltage sag (12%) in 2 cases: (A) FBL with PI tracking controller [10]. (B) FBL with PI+R tracking controller. (a). Grid voltage. (b). DC-link voltage. (c) Rotor current (d). Stator active power. (e). Stator reactive power. (f) Generator torque.

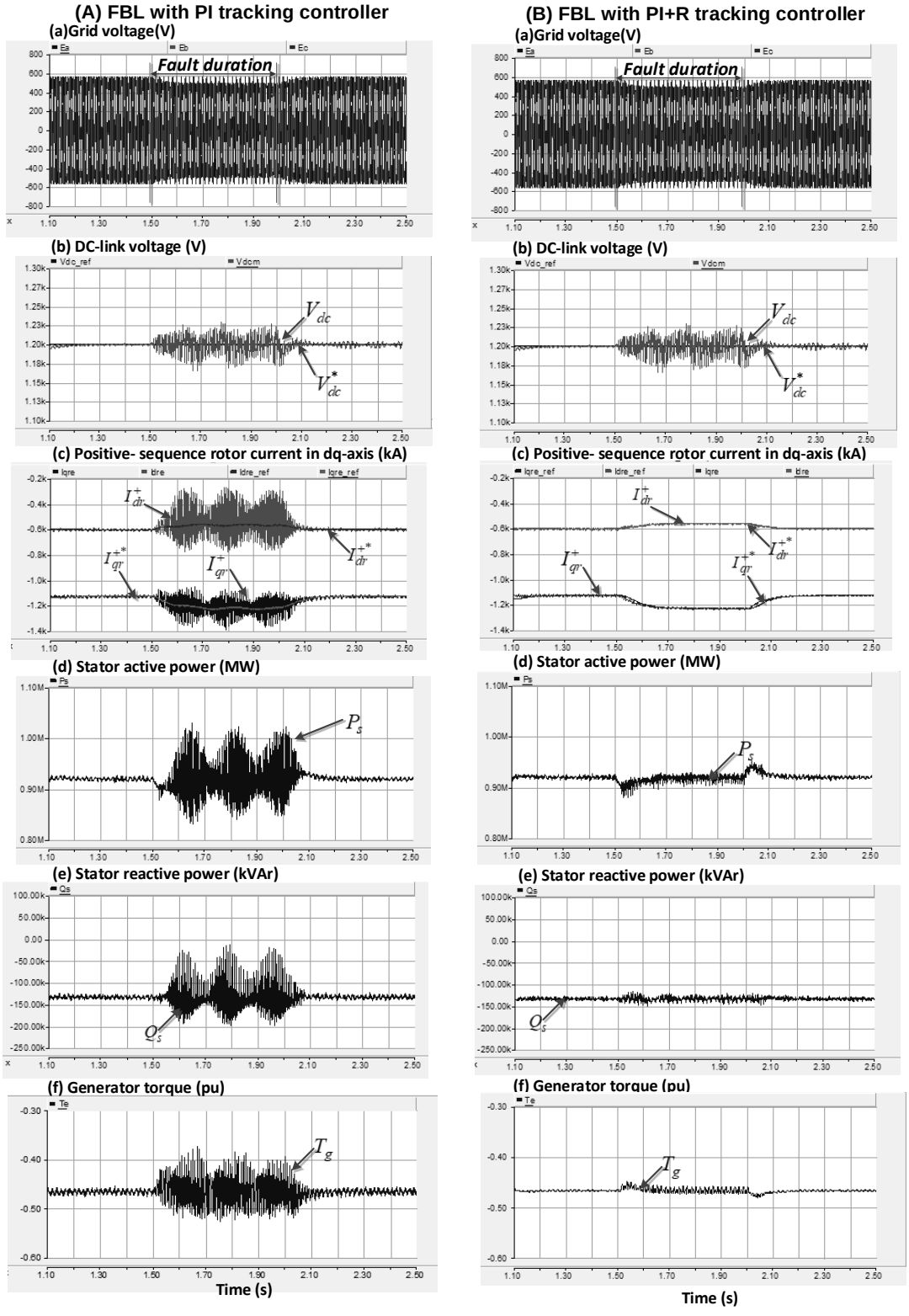

Figure 4. Wind generation performance for both grid phase-A and grid phase-B voltage sag (12%) in 2 cases: (A) FBL with PI tracking controller 10]. (B) FBL with PI+R tracking controller. (a). Grid voltage. (b). DC-link voltage. (c) Rotor current (d). Stator active power. (e). Stator reactive power. (f) Generator torque.

5. CONCLUSION

This paper has presented a current control scheme based on the feedback-linearization technique with the PI+R tracking controllers for the RSC of a DFIG wind turbine under unbalanced grid conditions. The dynamic response of the RSC of the DFIG to the transient grid unbalance has been analyzed and the current control scheme for RSC has been introduced. Compared with the existing unbalanced control method, the FBL with PI+R tracking controller one provides better performances for the rotor currents. The validity of the proposed one is verified by the simulation results for the 2 MW-DFIG wind turbine system under unbalanced grid voltage conditions.

REFERENCES

1. Pena R., Clare J. C., and Asher G. M. - Doubly fed induction generator using back-to-back PWM converter and its application to variable-speed wind-energy generation, IEE Proceedings on Electric Power Applications **143** (3) (1996) 231-241.
2. Yamamoto M. and Motoyoshi O. - Active and reactive power control for doubly-fed wound rotor induction generator, IEEE Transactions on Power Electronics **6** (4) (1991) 624-629.
3. Xu L. and Wang Y. - Dynamic modeling and control of DFIG-based wind turbines under unbalanced network conditions, IEEE Transactions on Power Systems **22 (**1) (2007) 314–323.
4. Brekken T. and Mohan N. - A novel doubly-fed induction wind generator control scheme for reactive power control and torque pulsation compensation under unbalanced grid voltage conditions, IEEE Power Electronics Specialists Conference Proceedings **2** (2003) 760-764.
5. Idsoe Nass B., Undeland T., and Gjengedal T. - Methods for reduction of voltage unbalance in weak gridsconnected to wind plants, Proceedings of IEEE Workshop Wind Power Impacts Power System, Oslo, Norway (2002) 17–18.
6. Lopez J., Gubia E., Sanchis P., Roboam X., and Marroyo L. - Wind turbines based on doubly fed induction generator under asymmetrical voltage dips, IEEE Transactions on Energy Conversion **23** (1) (2008) 321–330.
7. Brekken T. K. and Mohan N. - Control of a doubly fed induction generator under unbalanced grid voltage conditions, IEEE Transactions on Energy Conversion **22 (**1) (2007) 129–135.
8. Abo-Khalil A. G., Lee D.-C., and Jang J.-I. - Control of back-to-back PWM converters for DFIG wind turbine systems under unbalanced grid voltage, IEEE International Symposium on Industrial Electronics (2007) 2637–2642.
9. Hu J., He Y., and Wang H. - Adaptive rotor current control for wind-turbine driven DFIG using resonant controllers in a rotor rotating reference frame, Journal of Zhejiang University Science A **9** (2) (2008) 149–155.
10. Moon J.-W., Jin-Soo G., Park J.-W., Kang D.-W., and Kim J.-M. - Feedback linearization control of doubly-fed induction generator under an unbalanced voltage, 8th International Conference on Power Electronics - ECCE Asia, (2011) 662–669.

11. Djilali L., Sanchez E. N. and Belkheiri M. - Discrete-Time Neural Input Output Feedback Linearization Control for a DFIG based Wind Turbine, Proceedings of the 6th International Conference on Systems and Control (2017) 57-62.
12. Kim K.-H., Jeung Y.-C., Lee D.-C., and Kim H.-G. - LVRT scheme of PMSG wind power systems based on feedback linearization, IEEE Transactions on Power Electronics **27** (5) (2012) 2376-2384.
13. Van T. L., Nguyen T. D., Tran T. T., and Nguyen H. D. - Advanced control strategy of back-to-back PWM converters in PMSG wind power system, Advances in Electrical and Electronic Enginering (AEEE) - Power Enginering and Electrical Enginering **13** (2) (2015) 81-95.
14. Van T. L., Nguyen N. M. D., Toi L. T. and Trang T. T. - Advanced control strategy of dynamic voltage restorers for distribution system using sliding mode control input-ouput feedback linearization, Lecture Notes in Electrical Engineering **465** (2017) 521-531.

TÓM TẮT

CHIẾN LƯỢC ĐIỀU KHIỂN NÂNG CAO CỦA HỆ THỐNG TUA-BIN GIÓ DÙNG MÁY PHÁT DFIG KHI ĐIỆN ÁP LƯỚI KHÔNG CÂN BẰNG

Văn Tấn Lượng[1*], Phan Thị Chiêu Mỹ[2], Dương Văn Khải[1]
[1]*Trường Đại học Công nghiệp Thực phẩm TP.HCM*
[2]*Trường Đại học Văn Hiến*
*Email: *luonghepc@gmail.com*

Bài báo đề xuất kỹ thuật điều khiển phi tuyến nâng cao dựa trên sự kết hợp lí thuyết tuyến tính hóa hồi tiếp (FBL) và bộ điều khiển cộng hưởng, được gọi là bộ điều khiển giám sát, ở bộ nghịch lưu phía rotor (RSC) của hệ thống tua-bin gió dùng máy phát không đồng bộ nguồn kép (DFIG) khi điện áp lưới không cân bằng. Trước tiên, mô hình phi tuyến của hệ thống tua-bin gió dùng DFIG với bộ nghịch lưu phía rotor (RSC) được tuyến tính hóa, thay vì dùng phương pháp phân tích tín hiệu nhỏ phức tạp. Sau đó, bộ điều khiển tích phân-tỷ lệ và cộng hưởng (PI + R) được sử dụng như bộ điều khiển giám sát. Với sự kết hợp kỹ thuật tuyến tính hóa hồi tiếp và bộ điều khiển giám sát dựa trên bộ điều chỉnh cộng hưởng, các dao động của công suất và mô men máy phát được giảm nhiều ở cả ở trạng thái quá độ lẫn trạng thái xác lập. Kết quả mô phỏng hệ thống tua-bin gió máy phát DFIG với công suất 2 MW dùng phương pháp đề xuất đã được kiểm chứng trong trường hợp điện áp lưới không cân bằng.

Từ khóa: Điều khiển dòng điện, máy phát không đồng bộ nguồn kép, lí thuyết tuyến tính hóa hồi tiếp, điện áp lưới không cân bằng, tua-bin gió.